Journal of Computing and Electronic Information Management
ISSN: 2413-1660 | Vol. 21, No. 2, 2026

Design and Simulation of a 24 GHz Microstrip Array Antenna

Meilu Wang

Southwest Minzu University, Chengdu 610000, China

Abstract: To meet the demand for high gain and low sidelobe levels of array antennas in radar systems, hydrological monitoring, and next-generation wireless communication systems, this paper proposes a 24 GHz microstrip array antenna based on a series–parallel hybrid feeding network. The proposed design combines the advantages of both series and parallel feeding structures to optimize array performance while maintaining a compact configuration. Simulation results show that the antenna achieves a reflection coefficient better than −10 dB over the frequency range of 23.9–24.3 GHz, with a maximum gain of 19.58 dBi and a sidelobe level close to −20 dB. The results indicate that the proposed antenna can basically meet the design requirements for high gain and low sidelobe performance in radar systems.

Keywords: Microstrip Patch Antenna; High Gain; Low Sidelobe Level.

1. Introduction

Microstrip antennas have the advantages of low profile, lightweight structure, and good conformability. They can be easily integrated with RF circuits and active devices, and are suitable for mass production, offering significant benefits in reducing system cost[1-3]. Therefore, they have been widely used in radar systems, satellite navigation, mobile communications, and next-generation wireless communication systems. However, conventional microstrip antennas still suffer from narrow bandwidth, limited radiation efficiency and gain, as well as significant surface wave losses, which to some extent restrict their applications in broadband and high-performance systems[4]. Under the premise of maintaining these structural advantages, achieving effective sidelobe suppression through structural design and array synthesis has become an important research direction in the field of array antennas. The sidelobe level directly affects system anti-interference capability, angular resolution, and target detection performance, and is a key parameter in high-performance radar systems[5-8].

Due to their flexible structure and ease of array integration, microstrip antennas are commonly used as array elements to construct low-sidelobe antenna systems[9]. However, limited by the size and radiation mechanism of a single element, their gain and directivity are often insufficient to meet practical requirements. To address this issue, multiple antenna elements are typically arranged into a linear array with specific spacing and excitation, where coherent addition of radiated fields enhances the main lobe while suppressing sidelobes. On this basis, the structure can be further extended to a planar array, enabling two-dimensional beam control, higher gain, and flexible beam scanning. Therefore, planar arrays have significant application value in phased array radar, high-resolution imaging, and advanced communication systems[10-12].

2. Fundamentals of Array Antenna Theory

(1) Pattern Multiplication Theorem

The radiation performance of antenna arrays is closely related to several factors, including the type and number of array elements, element spacing, array configuration, as well as the amplitude and phase distribution of each element. Taking the simplest two-element array as an example, it consists of two closely spaced antenna elements with identical orientation, and can serve as a basic model for analyzing the radiation characteristics of antenna arrays.

Let the excitation current of element 1 be I_1, and that of element 2 be[13]:

$$I_2=mI_1e^{j\xi} \tag{1}$$

where m is the amplitude ratio and ξ is the phase difference.

Under far-field conditions, the radiation directions of the two elements are approximately identical, and the electric fields can be expressed as:

$$\vec{E}_1=\vec{e}_\theta j\frac{60I_1}{r_1}F_1(\theta,\phi)e^{-jkr_1} \tag{2}$$

$$\vec{E}_2=\vec{e}_\theta j\frac{60I_2}{r_2}F_2(\theta,\phi)e^{-jkr_2} \tag{3}$$

where:

$$F_1(\theta,\phi)=F_2(\theta,\phi)=\frac{\cos(kl\cos\theta)-\cos(kl)}{\sin\theta} \tag{4}$$

Using the far-field approximation $r_2\approx r_1-d\sin\theta\cos\phi$, we obtain:

$$\vec{E}_2=\vec{e}_\theta j\frac{60mI_1e^{j\xi}}{r_1}F_1(\theta,\phi)e^{-jk(r_1-d\sin\theta\cos\phi)}=m\vec{E}_1e^{j\psi} \tag{5}$$

$$\psi=kd\sin\theta\cos\phi+\xi \tag{6}$$

The total electric field at the observation point p is given by[13]:

$$\vec{E}=\vec{E}_1+\vec{E}_2=\vec{e}_\theta j\frac{60I_1}{r_1}F_1(\theta,\phi)e^{-jkr_1}\left(1+me^{j\psi}\right) \tag{7}$$

$$\left|\vec{E}\right|=\frac{60I_1}{r_1}F_1(\theta,\phi)\cdot f_a(\theta,\phi) \tag{8}$$

where $F_1(\theta,\phi)$ is the element pattern factor, and $f_a(\theta,\phi)=(1+m^2+2m\cos\psi)^{1/2}$ is the array factor. Equation (8) shows that the total radiation pattern of an antenna array can be expressed as the product of the element pattern and the array factor, which is known as the pattern multiplication theorem. This conclusion applies not only to two-element arrays but also to linear and planar arrays composed of identical or similar elements.

(2) Chebyshev Synthesis Method

In antenna array design, the main-lobe beamwidth and sidelobe level are generally in a trade-off relationship:

reducing the main-lobe beamwidth usually leads to an increase in sidelobe levels, while suppressing sidelobes may result in beam broadening. Therefore, a compromise optimization is required in engineering design to achieve the desired main-lobe beamwidth while minimizing the sidelobe level. The Chebyshev synthesis method can achieve an optimal weighting distribution under a specified sidelobe level constraint.

For a linear array consisting of N equally spaced elements, the array factor under Chebyshev weighting can be expressed as:

$$AF(u)=\sum_{n=1}^{M} I_n \cos[(2n-1)u] \quad (9)$$

$$u=\frac{kd}{2}\cos\theta \quad (10)$$

where $M=\frac{N}{2}$ (for even-numbered arrays), I_n is the weighting coefficient, and d is the element spacing. The formulation for odd-numbered arrays is similar. Through polynomial expansion, the array factor can be expressed as a function of $\cos(u)$, and then mapped to Chebyshev polynomials.

By specifying the main-to-sidelobe ratio R_0 in dB and converting it into its linear form, the following condition is obtained:

$$T_{N-1}(x_0)=R_0 \quad (11)$$

where $T_{N-1}(\cdot)$ denotes the Chebyshev polynomial of order N-1, and x_0 is the corresponding boundary parameter. By introducing the variable substitution $\cos(u)=\frac{x}{x_0}$, the array factor can be transformed into the standard Chebyshev form:

$$AF(u)=T_{N-1}(x) \quad (12)$$

Finally, the excitation amplitudes I_n of each element can be obtained by coefficient matching, thereby achieving the desired array weighting distribution that satisfies the target sidelobe level requirement.

3. Simulation Design of Microstrip Patch Antenna

(1) Antenna Element Design

The performance of a microstrip patch antenna is primarily determined by the geometry of the patch and the parameters of the dielectric substrate. After determining the substrate thickness and relative permittivity, the patch dimensions can be designed according to the target operating frequency to achieve good impedance matching and radiation performance. The initial formula for the patch width is given as:

$$W\_p=\frac{c}{2f_0}\left(\frac{\varepsilon_r+1}{2}\right)^{-\frac{1}{2}} \quad (13)$$

where c is the speed of light, f_0 is the target operating frequency, and ε_r is the relative permittivity of the substrate.

Considering the hybrid propagation of electromagnetic waves in both the dielectric substrate and air, an effective dielectric constant and fringing length correction are introduced as follows:

$$\varepsilon_{eff}=\frac{\varepsilon_r+1}{2}+\frac{\varepsilon_r-1}{2}\left(1+12\frac{h}{W\_p}\right)^{-\frac{1}{2}} \quad (14)$$

$$\Delta L=0.412h\frac{(\varepsilon_{eff}+0.3)\left(\frac{W\_p}{h}+0.264\right)}{(\varepsilon_{eff}-0.258)\left(\frac{W\_p}{h}+0.8\right)} \quad (15)$$

Thus, the actual patch length can be expressed as:

$$L\_p=L_{eff}-2\Delta L=\frac{\lambda_0}{\sqrt{\varepsilon_{eff}}}-2\Delta L=\frac{c}{2f_0}\frac{1}{\sqrt{\varepsilon_{eff}}}-2\Delta L \quad (16)$$

Under the operating frequency of 24.125 GHz, the initial patch dimensions are calculated using the above equations. Based on this, an inset-fed structure is introduced to construct the antenna element. Subsequently, an initial electromagnetic model is established in ANSYS HFSS, with appropriate boundary conditions and excitation settings. The antenna element model is shown in Figure 1.

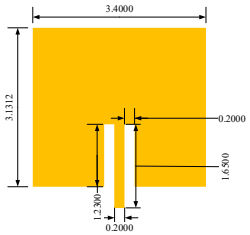

Figure 1. Microstrip antenna element model

The simulation results are shown in Figures 2 and 3. The antenna element exhibits a reflection coefficient better than −10 dB over the frequency range of 23.9–24.3 GHz, indicating good impedance matching and radiation performance within the target band. At 24.125 GHz, the maximum gain of the element is 5.70 dBi, which meets the design requirements. Based on this, through proper array configuration and feeding network design, the array superposition effect can be utilized to further enhance the overall antenna gain, thereby satisfying the high-gain requirements of the array system.

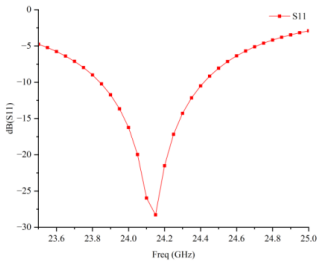

Figure 2. Simulated S11 Curve of the Antenna Element

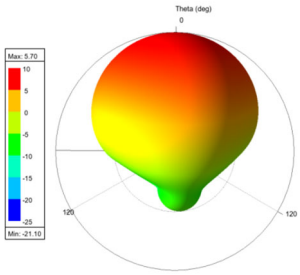

Figure 3. 3D Radiation Pattern of the Antenna Element

(2) Array Design

In the feeding network design, the Dolph-Chebyshev weighting model is adopted. By applying Barbil's formulas (17) and (18) and using MATLAB for calculation, the excitation amplitude coefficients of each array element are obtained.

$$I_i=\sum_{q=i}^{N}(-1)^{N-q}x_0^{2q-1}\frac{(2N-1)(q+N-2)!}{(q-i)!\,(q+i-1)!\,(N-q)!} \quad (17)$$

$$I_i=\sum_{q=i}^{N}(-1)^{N-q}x_0^{2q}\frac{(2N)(q+N-2)!}{(q-i)!\,(q+i-1)!\,(N-q)!} \quad (18)$$

where I_i is the excitation amplitude of the i-th element, N is the number of elements in half of the array, and q is the index parameter in the weighting distribution. This method enables the array radiation pattern to satisfy the prescribed Chebyshev sidelobe level constraint.

To avoid grating lobes, the element spacing must satisfy:

$$d<\frac{\lambda_0}{1+|\sin\theta_0|} \quad (19)$$

where θ_0 is the maximum scanning angle and λ_0 is the free-space wavelength at the operating frequency.

In this design, beam scanning is not required; therefore, the element spacing only needs to satisfy the grating-lobe-free condition. The characteristic impedance of the microstrip feed line is set to a fixed value, and impedance transformation sections are introduced at the front of each element to achieve impedance matching and power division, ensuring accurate amplitude and phase excitation for each element and thus guaranteeing overall array performance. Through optimized design of the feeding network parameters, the power distribution is properly controlled so that the excitation amplitudes follow the Chebyshev weighting distribution. Considering the symmetry of the array structure, only half of the feeding network needs to be analyzed to derive the performance of the entire array. Based on the Chebyshev synthesis method with a sidelobe level of −20 dB, the excitation current ratios of each port are calculated, and the corresponding microstrip line impedances are derived inversely to determine the geometrical dimensions of the feed network. A 1-to-8 power divider network is thus designed, as shown in Figure 4. Similarly, a 1-to-4 power divider structure is obtained, as shown in Figure 5.

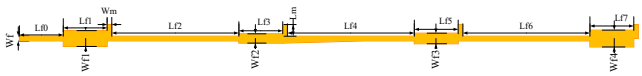

Figure 4. 1-to-8 Power Divider Network Structure and Dimensions (Half Structure)

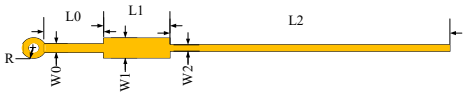

Figure 5. 1-to-4 Power Divider Network Structure and Dimensions (Half Structure)

Based on the simulation analysis of the single-row linear array, the array structure is further extended by increasing the number of rows of microstrip arrays to form a planar array. Meanwhile, the connection scheme between different rows of the main feed line and the corresponding impedance matching structures are optimized to achieve a co-optimized design of the array structure and feeding network. As a result, a 4×8 microstrip patch array model is obtained, as shown in Figure 6.

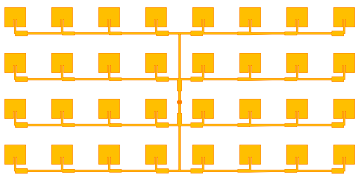

Figure 6. Overall Antenna Structure

(3) Planar Array Optimization Analysis

ANSYS HFSS is used to perform parametric optimization of the array antenna. The main variables include the patch element length, the main feed line width W1, and the element spacing d.

Variations in patch length affect the effective electrical length of the antenna, thereby causing a shift in the resonant frequency: as the length increases, the resonant frequency shifts toward lower frequencies. Meanwhile, this parameter also influences the radiation pattern of the element, which in turn affects the overall radiation performance of the array, including the main-lobe beamwidth and sidelobe distribution. figures 7 and 8 present the variations of S-parameters and radiation patterns under different patch lengths. The simulation results show that when the patch length is set to 3.1312 mm, the array antenna achieves the best impedance matching performance, with a reflection coefficient better than −30 dB, while also obtaining the maximum gain.

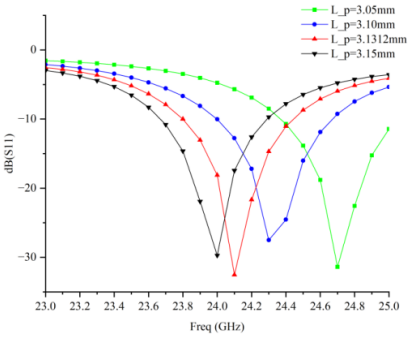

Figure 7. Effect of L_p on S11

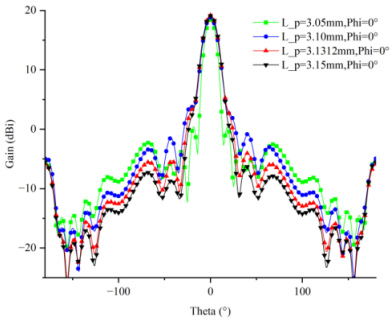

Figure 8. Effect of L_p on the Antenna Radiation Pattern

Through parameter sensitivity analysis, it is found that among the key structural parameters, the main feed line width W1 has a significant impact on antenna performance, primarily reflected in variations of the reflection coefficient and the depth of the resonant response. Figure 9 shows the parameter variations under different values of W1. Considering both impedance matching performance and design margin, the main feed line width W1 is finally determined to be 0.63 mm to achieve improved impedance matching characteristics and stable operating performance.

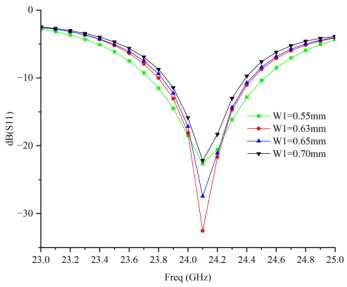

Figure 9. Effect of Main Feed Line Width W1 on Antenna Performance

In the process of extending the linear array to a planar array, the element spacing d has a significant impact on the performance of the planar array antenna, and its value should be determined according to the design requirements. First, an initial spacing is determined based on $\lambda_0 = c/f_0$, and then further optimized through simulations. figures 10 and 11 show the effects of different element spacing values d on the antenna reflection coefficient and radiation pattern, respectively.

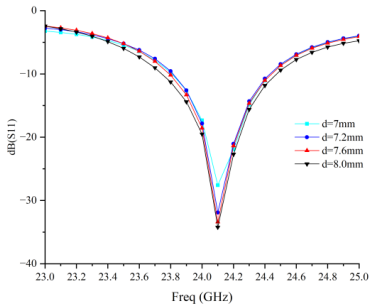

Figure 10. Effect of d on S11

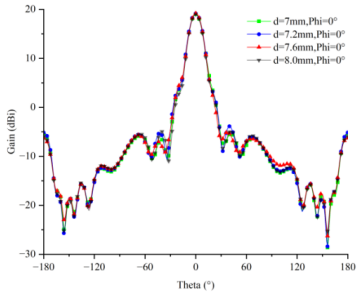

Figure 11. Effect of d on the Antenna Radiation Pattern

Variations in the element spacing d affect the antenna input impedance through mutual coupling between array elements, thereby influencing the reflection coefficient. Under the condition of avoiding grating lobes, simulation results show that appropriately increasing the element spacing can improve impedance matching at the operating frequency, resulting in a lower reflection coefficient and reduced power reflection, while the variation in array gain remains relatively small. Considering both impedance matching and radiation characteristics, the element spacing is finally selected as d=7.6 mm.

(4) Simulation Results Analysis

The 4×8 microstrip array antenna is designed, simulated, and optimized using ANSYS HFSS to ensure that its center frequency, operating bandwidth, gain, and sidelobe suppression performance meet the requirements of wireless transmission systems. The simulation results are shown in Figures 12 and 13.

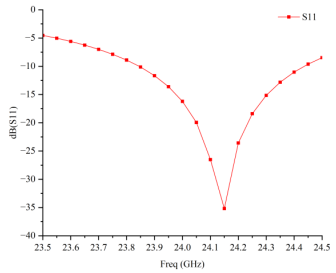

Figure 12. S11 Curve of the 4×8 Microstrip Array Antenna

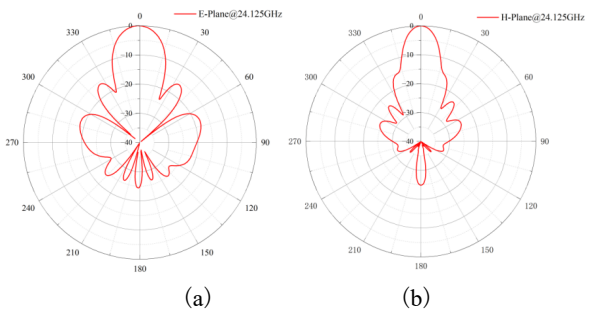

(a) (b)

Figure 13. Radiation Patterns of the Array Antenna: (a) E-plane, (b) H-plane

The results indicate that within the frequency range of 23.9-24.3 GHz, the array antenna exhibits a reflection coefficient better than -10 dB, reaching -36 dB at 24.125 GHz, which demonstrates good impedance matching performance. In addition, the radiation pattern shows that the maximum gain of the array is 19.58 dBi, and the sidelobe level is close to -20 dB. These results confirm that the proposed antenna meets the high-gain and low-sidelobe requirements of radar systems, thereby validating the rationality and feasibility of the designed array structure and feeding network.

4. Conclusion

This paper focuses on the requirements of 24 GHz radar applications and designs a 4×8 microstrip patch array antenna based on a series–parallel hybrid feeding network. By analyzing the fundamental theory of array antennas, the pattern multiplication theorem and the Chebyshev synthesis method are introduced to optimize the amplitude distribution of the array. Meanwhile, the structural parameters of the microstrip patch antenna element and electromagnetic simulations are combined to systematically optimize key dimensional parameters and the feeding network. The array performance is improved while maintaining a compact antenna structure.Simulation results show that within the target operating frequency band, the antenna exhibits a reflection coefficient better than -10 dB, a maximum gain of 19.58 dBi, and a sidelobe level close to -20 dB. The results indicate that the proposed array antenna meets the design requirements and can enhance the overall performance of radar systems.

References

[1] Sengupta, S., Jackson, D. R., & Long, S. A. (2015). A method for analyzing a linear series-fed rectangular microstrip antenna array. IEEE Transactions on Antennas and Propagation, 63(8), 3731-3736. https://doi.org/10.1109/TAP.2015.2434404

[2] Dzagbletey, P. A., & Jung, Y. B. (2018). Stacked microstrip linear array for millimeter-wave 5G baseband communication. IEEE Antennas and Wireless Propagation Letters, 17(5), 780-783. https://doi.org/10.1109/LAWP.2018.2817019

[3] Sugawa, S., Sakakibara, K., Kikuma, N., & Hirayama, H. (2012). Low-sidelobe design of microstrip comb-line antennas using stub-integrated radiating elements in the millimeter-wave band. IEEE Transactions on Antennas and Propagation, 60(10), 4699-4709. https://doi.org/10.1109/TAP.2012.2207338

[4] Hayashi, Y., Sakakibara, K., Nanjo, M., Kikuma, N., & Hirayama, H. (2011). Millimeter-wave microstrip comb-line antenna using reflection-canceling slit structure. IEEE Transactions on Antennas and Propagation, 59(2), 398-406. https://doi.org/10.1109/TAP.2010.2096196

[5] Babas, D. G., & Sahalos, J. N. (2007). Synthesis method of series-fed microstrip antenna arrays. Electronics Letters, 43(2), 78-80. https://doi.org/10.1049/el:20073453

[6] Yin, J., Wu, Q., Yu, C., Wang, H., & Hong, W. (2017). Low-sidelobe-level series-fed microstrip antenna array of unequal interelement spacing. IEEE Antennas and Wireless Propagation Letters, 16, 1695-1698. https://doi.org/10.1109/LAWP.2017.2669985

[7] Xu, T. M., Yao, M. L., Zhang, F. G., Liu, Y., & Liu, B. (2020). Design of low sidelobe series microstrip array antenna with non-uniform spacing and excitation amplitude. Electronics Letters, 56(21), 1099-1101.

https://doi.org/10.1049/el.2020.2200

[8] Kahrizi, M., Sarkar, T. K., & Maricevic, Z. A. (1993). Analysis of a wide radiating slot in the ground plane of a microstrip line. IEEE Transactions on Microwave Theory and Techniques, 41(1), 29-37. https://doi.org/10.1109/22.210227

[9] Ding, J., Lin, Z., Ying, Z., & He, S. (2007). A compact ultra-wideband slot antenna with multiple notch frequency bands. Microwave and Optical Technology Letters, 49(12), 3056-3060. https://doi.org/10.1002/mop.22897

[10] Li, X. (2016). Design of a broadband microstrip array antenna in X-band. Wireless Communication Technology, 25(1), 41-45, 49.

[11] Richards, W. F., Lo, Y. T., & Harrison, D. D. (1981). An improved theory for microstrip antennas and applications. IEEE Transactions on Antennas and Propagation, 29(1), 38-46. https://doi.org/10.1109/TAP.1981.1142524

[12] Yang, Q. (2014). Key technologies of a C-band circularly polarized broadband monopulse microstrip array antenna [Master's thesis]. Beijing Institute of Technology.

[13] Xie, C., & Rao, K. (2006). Electromagnetic fields and electromagnetic waves (4th ed.). Higher Education Press.